Skinny fat model of metabolic syndrome induced by a high-salt/sucrose diet in young male rats

Keilah Valéria Naves **Cavalcante**[1]; Marcos Divino **Ferreira-Junior**[1]; Marina Conceição dos Santos **Moreira**[2]; Stefanne Madalena **Marques**[3]; James Oluwagbamigbe **Fajemiroye**[4]; Rosiane Aparecida **Miranda**[5]; Patrícia Cristina **Lisboa**[5]; Egberto Gaspar de **Moura**[5]; Carlos Henrique **Xavier**[6]; Eduardo **Colombari**[7]; Rodrigo Mello **Gomes**[1,#] and Gustavo Rodrigues **Pedrino**[3,#,*]

[1]Laboratory of Endocrine Physiology and Metabolism, Federal University of Goiás, GO, Brazil.

[2]Department of Academic Areas, Federal Institute of Education, Science, and Technology of Goiás, Campus Formosa, GO, Brazil.

[3]Neuroscience and Cardiovascular Physiology Research Center, Federal University of Goiás, GO, Brazil.

[4]Department of Pharmacology, Federal University of Goiás, GO, Brazil.

[5]Laboratory of Endocrine Physiology, State University of Rio de Janeiro, Rio de Janeiro, RJ, Brazil.

[6]Systems Neurobiology Laboratory, Federal University of Goiás, GO, Brazil.

[7]Department of Physiology and Pathology, School of Dentistry, São Paulo State University, UNESP, Araraquara, SP, Brazil.

#These *authors contributed equally to this manuscript.*

This peer-reviewed article has been accepted for publication but not yet copyedited or typeset, and so may be subject to change during the production process. The article is considered published and may be cited using its DOI

10.1017/S0007114524002927

The British Journal of Nutrition is published by Cambridge University Press on behalf of The Nutrition Society

*__Corresponding author:__ Gustavo Rodrigues Pedrino, Department of Physiological Sciences, Biological Sciences Institute II, Room 107, Federal University of Goiás, Esperance Avenue, CEP: 74690-900, Goiânia/GO, Brazil.
E-mail: pedrino@ufg.br (G. R. Pedrino).

Short title: High salt and sucrose levels affect BAT function.

List of abbreviations

Adrenergic β-3 Receptor (β3-AR)
Alanine Aminotransferase (ALT)
Aspartate Aminotransferase (AST)
Body Mass Index (BMI)
Body Weight (BW)
Brown Adipose Tissue (BAT)
Control Group (CO)
Electrocardiography (ECG)
Epididymal (e)
Glucose Tolerance Test (oGTT).
Hematoxylin and Eosin (HE)
High-Density Lipoprotein (HDL)
High-Sodium/Sucrose Diet Group (SS)
Insulin Tolerance Test (ipITT).
Intraperitoneal (ip)
Intravenous (iv)
Peroxisome Proliferator-Activated Receptor Gamma (PPARγ)
Peroxisome Proliferator-Activated Receptor Alpha (PAPR-α)
Retroperitoneal (rp),
Standard Error of the Mean (SEM)
Subcutaneous (sc)
Triglycerides (TGs)
Uncoupled Protein (UCP-1)
White Adipose Tissue (WAT)

ABSTRACT

Childhood and puberty can affect metabolism, leading to tissue injury and malfunction later in life. The consumption of high-processed foods rich in salt and sugar is increasing in middle- and high-income countries, especially among young people. It is necessary to evaluate the effects of high salt and sugar levels in the youth on most injured organs during metabolic challenges. We aimed to investigate whether high salt/sucrose intake affects whole-body development and leads to end-organ injury. Weaned Male Wistar rats were divided into two groups: a control group fed a standard diet (CO) and tap water, and an experimental group (SS) fed a standard diet and a beverage containing 1.8% NaCl and 20% sucrose instead of tap water. The animals were treated for 60 days, starting after weaning at 21 days of age, after which the animals were subjected to glucose and insulin tolerance tests, urine collection, and heart rate monitoring, and euthanized for sample collection at 81 days of age. SS showed reduced body weight gain and increased food intake of sodium/sucrose solution. Interestingly, high salt/sucrose intake led to increased body adiposity, liver lipid inclusion, heart rate, and renal dysfunction. SS exhibits increased levels of peroxisome proliferator-activated receptor alpha to counterbalance the hypertrophy of brown adipose tissue. Our findings reveal that the SS rat model exhibits non-obvious obesity with end-organ damage and preserved brown adipose tissue function. This model closely parallels human conditions with normal BMI but elevated visceral adiposity, providing a relevant tool for studying atypical metabolic disorders.

Keywords: Renal failure; Liver lipid accumulation; Cardiometabolic disease; Early life nutrition; Tachyarrhythmia.

1. INTRODUCTION

Childhood and puberty are life stages characterized by transitions and the formation of dietary patterns. Unhealthy food intake patterns among children and adolescents, as well as insufficient physical activity, contribute to overweight and obesity in this life stage and increase the risk of non-communicable diseases later in life. Although obesity is easily diagnosed by the well-standardized Body Mass Index (BMI), some individuals are known to have skinny fat, which shows metabolic obesity but an average weight[1,2].

An unhealthy diet is one of the factors contributing to the development of obesity, commonly due to an overload of sugar or fat in the diet. The consumption of ultra-processed foods is rapidly increasing in middle- and high-income countries [3]. Studies using animal models have shown that rats fed a diet rich in carbohydrates such as sucrose experience an increase in body adiposity[4]. Variations in diet composition change the way energy is used, which can lead to an increase in fat deposits[5]. Tenk e Felfeli[6] observed that, similar to humans, rats also show a higher intake of processed foods with a high fat and/or sugar content due to the high palatability of the food.

Excess dietary sodium is linked to several pathologies, including heart damage and kidney injury, leading to morphological alterations in these tissues. Recently, it has been demonstrated that high sodium intake during puberty leads to hypertension and cardiac remodeling in adulthood[7]. In addition, high dietary sodium levels during puberty induce short-term cardiac and renal effects[8].

Excessive carbohydrate intake promotes lipogenesis, a process by which triglycerides are formed from excess glucose and processed by the liver and adipose tissues [9,10]. Thus, in addition to the consequences of these changes in glucose metabolism, the liver participates in pathophysiological mechanisms of fat accumulation [11,12]. An increase in sugar intake leads to obesity and the development of ectopic lipid storage in the liver[13]. Increased lipogenesis and hypertriglyceridemia result in greater adiposity and hypertrophy of white adipose tissue (WAT)[14–16]. Brown adipose tissue (BAT) plays a crucial role in thermogenesis; thus, its adipocytes have a different morphology than WAT adipocytes. However, during the onset of obesity, BAT adipocytes change their morphology and metabolism, assuming a white adipocyte phenotype, among which we can highlight a more significant deposition of triglycerides and cell hypertrophy[16–18]. In BAT, uncoupled protein (UCP-1) is expressed as a thermogenic function, and the adrenergic β-3 receptor (β3-AR) pathway is essential for

thermogenesis[16,19]. β3-AR stimuli trigger the cAMP-dependent protein kinase signaling cascade that results in lipolysis of triglycerides (TGs) from BAT and mitochondrial β-oxidation, resulting in thermogenesis[20]. Peroxisome proliferator-activated receptor-α (PAPR-α) plays an essential role in BAT function, with potential effects on thermogenesis and browning, as well as High-Density Lipoprotein (HDL) and TGs blood levels[21,22].

Although the effects of high-salt/sugar diets during adulthood are well-defined in the literature, little is known about the role of the early stages of life in the development of diseases in adulthood. In the present study, we aimed to investigate whether high sodium/sucrose intake during the first stages of life affects whole-body development and leads to end-organ injury.

2. MATERIAL AND METHODS

All protocols were approved by the Ethics Committee on the Use of Animals of the Federal University of Goiás (CEUA/UFG; protocol number 023/15) and carried out in accordance with the standards recommended by the Brazilian Animal Experimentation Control Council (CONCEA) and Animal Research: Reporting of In Vivo Experiments (ARRIVE) guidelines for scientific research.

2.1. Animals and diets

21-day-old weaned male Wistar rats were housed and cared for at the Animal Facility of the Department of Physiological Sciences, Federal University of Goiás. The rats were maintained under controlled conditions, with a 22 ± 2 °C temperature and a 12/12 h light/dark cycle. Each rat was housed in polypropylene cages with environmental enrichment appropriate for rodents. The cages were cleaned regularly, and the bedding, composed of wood shavings valued for their absorbent properties and low dust content, was replaced twice a week to maintain a clean and comfortable environment. The animals were allocated into two experimental groups: i. the control group (CO; n = 14), which received tap water filtered through activated carbon, and ii. the high-sodium/sucrose group (SS; n = 14), which was administered a solution containing 1.8% (w/v) NaCl (Synth, Diadema, SP, Brazil) and 20% (w/v) sucrose (Synth, Diadema, SP, Brazil), diluted in tap water filtered through activated carbon. This protocol was based on previous studies utilizing high-sodium solutions[7,8] and high-sucrose diets[23,24]. Animals were fed their diets for 60 days from weaning (21-day-old)

until 81-day-old and had unlimited access to standard chow (Nuvilab; Colombo, Paraná, Brazil) and water. At the end of the experimental period, all the groups received tap water and were fed a standard diet. Body weight and food intake were measured every week. Lee index was calculated, according to previous work, briefly as a ratio between the cubic root of body weight and the nasoanal length[25]. Here, we only used male rats to avoid sex hormone-induced confounding factors. Caloric intake of carbohydrates, sodium, protein, and fat was estimated using the information provided by the standard chow manufacturer and the concentration of sodium and sucrose in the solution offered to the SS group.

2.2. Glucose homeostasis assessment

At the end of the experimental period, a batch of animals from both groups (n = 6 per group) was fasted for 12 h to perform the oral Glucose Tolerance Test (oGTT). Initially, a blood sample was collected for basal glycemia at 0 min. A glucose solution (2 g/kg of BW) was injected orally. Blood samples were collected at 60 and 120 min after glucose injection. Blood samples were collected through a small puncture at the tip of the tail, and blood glucose levels were measured using a commercial glucometer (On Call Plus, San Diego, California, USA).

The next day, the animals used in the oGTT were subjected to an intraperitoneal Insulin Tolerance Test (ipITT). The food was removed two hours before the protocol was performed. As in the oGTT, a blood sample was collected to measure basal glycemia at time 0. Fast-acting insulin solution (2 U/kg of the BW, ip) Eli Lilly, São Paulo, Brazil) was administered intraperitoneally. Caudal blood samples were collected 10, 20, and 30 min after insulin injection. Blood glucose levels were measured using a commercial glucometer (On Call Plus, San Diego, California, USA).

The animals used for the glucose homeostasis assessment were euthanized after the experiments and were not used for further analysis.

2.3. Renal and cardiac assessments, euthanasia, and sample collection

At the end of the experimental period, another batch of animals (n = 8 per group) was placed in a metabolic cage for 12 hours to collect the urine. After 12h of acclimation, urine of 12h was collected. Tap water and standard rodent chow were used in this study. The animals were then moved to their cages, and the next day, they were dressed in an acquisition jacket,

and electrocardiography (ECG) was performed. Ten minutes of acclimatization were followed by five minutes of acquisition. Data from the ECG were amplified (1000x) and acquired at 1 kHz (ADInstruments, USA) and used to calculate the heart rate from RR intervals (Powerlab, ADInstruments, USA).

After ECG, the animals were fasted overnight and anesthetized with sodium thiopental (40 mg/kg of the BW, ip; Thiopentax, Cristália, São Paulo, Brazil). Blood samples were collected from the inferior vena cava using a sterile needle and syringe, centrifuged for plasma collection (3000 × g, 15 min), and stored at -20 °C. The pancreas, liver, kidney, heart, adrenal glands, BAT, retroperitoneal (rp), epididymal (e), and inguinal subcutaneous (sc) WAT were dissected and weighed.

2.4. Biochemical assays and calculations

Levels of Aspartate aminotransferase (AST), alanine aminotransferase (ALT), and plasmatic/urinary creatinine were measured by enzymatic-colorimetric methods using a commercial kit (DOLES, Goiânia, Brazil) following the manufacturer's instructions.

The glomerular filtration rate was calculated according to a previous study[26] using the following formula: [(Urinary Creatinine × Urinary Flow)/Plasma Creatinine]. Urinary Flow was calculated as the ratio of the total volume of urine collected at the time of collection (in min).

2.5. Western blot

BAT samples (n = 4 per group) were homogenized in ice-cold RIPA lysis buffer and centrifuged (12000 × g, 4 °C) to collect the supernatant. Protein concentrations were determined using the Bradford protein quantification assay. The samples were denatured in Laemmli buffer and heated at 95 °C for 3 min. SDS-PAGE separated aliquots of 15 µg protein from each sample and then transferred them to nitrocellulose membranes. The membranes were incubated with blocking solution (5% skim powdered milk, 10 mM Tris, 150 mM NaCl, and 0.02% Tween 20) under mild agitation for 90 min at room temperature. Subsequently, the membranes were washed with Tris-buffered saline and incubated overnight at 4 °C with the primary antibodies anti-β3AR (#sc-515763), anti-UCP-1 (#sc-518024), anti-Peroxisome proliferator-activated receptor alpha (PPARα; #sc-398394), anti-peroxisome proliferator-activated receptor gamma (PPARγ; #sc-7273), anti-AKT (#sc-81434), and anti-

pAKT (#sc-7985), following manufacturer instructions. The membranes were then gently washed (3x 5 min; 10 mM Tris, 150 mM NaCl, and 0.02% Tween 20) and incubated with the appropriate HRP-conjugated secondary antibody for 90 min. The protein bands were visualized using chemiluminescence (ECL kit; Amersham Biosciences, London, UK) and exposed to ImageQuant LAS (GE Healthcare, Buckinghamshire, UK). The area and density of the bands were quantified using ImageJ software (NIH, MA, USA). β-Actin was used as a load control.

2.6. Histological analysis

The pancreas, liver, kidney, heart, and BAT samples were fixed in 10% formaldehyde for 24 hours and stored in 70% alcohol. The samples were then dehydrated, diaphanized in xylol, and embedded in histological paraffin (Synth, Diadema, São Paulo, Brazil). Subsequently, the material was sectioned at a thickness of 5 µm using a microphone (RM2245; Leica Microsystems, Wetzlar, Germany). The sections were stained with hematoxylin and eosin (pancreas, liver, kidney, and BAT), or picrosirius red for collagen staining (heart).

2.7. Measurement of the cardiomyocyte diameter, pancreatic islets, brown adipocyte, and glomerular areas

Photomicrographs of the cross-sections of the left ventricular cardiomyocytes were analyzed according to a previous study [27]. The distance between the upper and lower parts of the cell membrane was measured at the height of the nucleus in each cardiomyocyte. Measurements were made at four different points in the middle layer of each cut and in three different cuts to assess the thickness of the intima-media layer. The mean cardiomyocyte diameter for each animal was calculated, and the results were compared between groups.

Pancreatic islets, brown adipocytes, and glomerular areas were measured using at least 20 measurements from three different cuts per animal. The mean values were calculated for each animal, and the results were compared between the groups.

For these image analyses, the ICY Image Analysis software was used (Institut Pasteur, Paris, France). <http://icy.bioimageanalysis.org/>).

2.8. Interstitial fibrosis measurement

Interstitial fibrosis was analyzed by macro-processing using FIJI (v1.54f, ImageJ). Briefly, the images were processed using color deconvolution to split the hematoxylin and picrosirius red staining components. The picrosirius red channel was subjected to a threshold for evidence of actual staining areas. The marked areas were then quantified. The percentage of interstitial fibrosis was estimated as the ratio of the marked area to the total area of the image. The mean and standard error of the mean of the percentage of Interstitial Fibrosis were calculated for each animal, and the results were compared between the groups.

2.9. Liver lipid inclusion

To evaluate liver lipid inclusion, stereological analysis was performed on HE-stained sections (1000x magnification), with a mesh of 594 points. At least ten slices from each animal were used. The mean value of lipid inclusion for each animal was calculated, and the results were compared between groups.

Stereological analysis was performed using Image-Pro Plus software (version 6.0; Media Cybernetics, Rockville, MD, USA).

2.10. Statistical analysis

The sample size was calculated *a priori* using G*Power (v3.1). Based on previous reports [7,8,24,28], our first outcome was increasing dietary sodium and sucrose intake. For this purpose, a minimum variation of 25% in the intake of the offered solution was expected. With a power of 80% and a significance level of 5%, this allowed the detection of a difference of 20% between the groups, with a minimum sample size of eight animals/group.

Data are expressed as mean ± standard error of the mean (SEM). Unpaired Student's t-test was used to compare differences between groups. Two-way ANOVA was used to compare the differences in body weight, food intake, ivGTT, and ipITT curves, followed by the Sidak post-hoc test. Simple linear regression was used to perform the correlation analysis. Prism version 9.01 software (GraphPad, San Diego, CA, USA) was used for the data analysis and graphical construction. Differences were considered statistically significant at $p<0.05$.

3. RESULTS

3.1. SS diet impacts body development and increases adipose tissue weight.

The SS group exhibited delayed body weight gain throughout the experimental period (Fig. 1A). In addition, owing to the increased intake of high-sucrose and sodium mixtures (Fig. 1B), and food intake was reduced in these animals (Fig. 1C) than in the CO group. At the end of the experimental period, the SS group had increased carbohydrate levels (CO 0.384 ± 0.012 vs. SS 0.707 ± 0.029 g/b. wt./week; <0.0001; Fig. 1D) and sodium intake (CO 0.18 ± 0.007 *vs.* SS 6.85 ± 0.250 g/week; p<0.0001; Fig. 1E); however, due to the decreased chow intake, they reduced the weekly intake of proteins (CO 0.0698 ± 0.003 *vs.* SS 0.0511 ± 0.005 g/b. wt./week; p=0.0051; Fig. 1F) and fat (CO 0.0222 ± 0.0009 *vs.* SS 0.0163 ± 0.0016 g/b.wt./week; p=0.0051; Fig. 1G). Overall caloric intake did not differ between the groups (Fig. 1H).

At the end of the experimental period, the body weight (CO 315.3 ± 11.3 vs SS 196.4 ± 8.95 g; p<0.001; Fig. 1I), nasoanal length (CO 20.4 ± 0.27 SS 17.5 ± 0.39 cm; p<0.001; Fig. 1J), and tibia length (CO 3.77 ± 0.034 vs SS 3.27 ± 0.0348 cm; p<0.0001; Fig. 1K) were reduced in SS group. However, despite lower body weight, the adiposity in the SS group was higher than in the CO group, indicated by retroperitoneal (CO 466.3 ± 60.46 *vs* SS 1125.0 ± 87.01 mg/100 g b.wt.; Fig. 1L), epididymal (CO 547.8 ± 62.32 *vs* SS 932.8 ± 103.70 mg/100 g b.wt.; Fig. 1M) and subcutaneous (CO 282.7 ± 38.32 *vs* SS 583.0 ± 63.11 mg/100 g b.wt.; Fig. 1N) fat pads increased the relative weight. In contrast, the Lee index was similar between groups (Fig. 1).

3.2. SS diet correlates with increased white and brown adipose tissue weight.

Similar to the CO group, we found that the SS group had a positive correlation between adipose tissue weight and body weight. However, despite a positive correlation, the retroperitoneal, epididymal, and subcutaneous fat pads presented left-displaced values in the SS group compared with those in the CO group (p<0.001; Fig. 2A-C). Regarding brown adipose tissue, there was a strong correlation with the body weight in SS animals, with BAT weights higher than those in CO animals (p=0.002; Fig. 2D). Similarly, the adrenal gland presented a positive correlation with body weight in both CO and SS animals; however, SS animals were more prone to show a slightly increased adrenal weight (p=0.028; Fig. 2E).

There was a weak correlation between tibia length and body weight in SS animals (p=0.032; Fig. 2F) compared to that in CO.

3.3. SS diet does not affect glucose homeostasis but leads to hepatic lipid inclusion.

There was no significant difference between the groups during the oGTT (Fig. 3A and 3E) and ITT (Fig. 3B and 3F). In addition, we observed that the basal blood glucose levels are similar under long (CO 64.7 ± 2.40 *vs* SS 64.6 ± 4.82 mg/dL; Fig. 3A) and short fasting (CO 93.0 ± 5.83 *vs* SS 91.2 ± 6.64 mg/dL; Fig. 3B). Despite the higher values of normalized pancreas weight (CO 168.7 ± 6.202 vs. SS 226.4 ± 14.13 mg/100 g b.wt.; p=0.0015; Fig. 3C), SS animals showed no difference in pancreatic islet area compared to the control group (Fig. 3D).

The SS diet also affected the normalized liver weight (CO, 3720 ± 167.7 vs. SS 4297 ± 155.7 mg/100 g; p<0.05; Fig. 3G) and hepatic lipid accumulation (CO 0.4 ± 0.04% vs. SS 2.5 ± 0.25%; p<0.0001; Fig. 3H) compared to the CO diet; however, no difference was detected in plasma markers of hepatic injury (Fig. 3 I-J).

3.4. SS diet affects renal function and increases heart rate.

Despite increased normalized kidney weight (CO 347.1 ± 6.63 *vs* SS 419.2 ± 17.77 mg/100 g b.wt.; p<0.01; Fig. 4A), the SS animals had lower glomerular (CO 5555 ± 266.1 vs SS 3567 ± 189.2 μm^2; p<0.001; Fig. 4B) and capsular space (CO 1136.0 ± 124.10 vs SS 779.8 ± 68.27 μm^2; p<0.05; Fig. 4C) areas compared to CO animals, as well as pericapsular collagen marking in the glomeruli (CO 6762 ± 342.1 vs SS 4411 ± 237.1 μm^2; p<0.01; Fig. 4D). In parallel to those morphologic changes, the SS group exhibits impaired urinary function, marked by lower creatinine clearance (Urinary; CO 71.71 ± 7.368 vs SS 22.28 ± 5.025 mg/dL; p<0.0001; Fig. 4E / Plasmatic; CO 0.42 ± 0.074 vs SS 0.65 ± 0.052 mg/dL; p<0.05; Fig. 4F), lower glomerular filtration rate (CO 15.160 ± 5.717 vs SS 0.775 ± 0.4305 ml/min; p=0.0360; Fig. 4G) and urinary flow (CO 0.050 ± 0.0051 vs SS 0.023 ± 0.0079 ml/min; p<0.05; Fig. 4H).

In addition to renal effects, the SS diet also affects the heart. The SS group present lower normalized heart weight (CO 316.1 ± 14.64 vs SS 242.3 ± 15.06 mg/100 g b.wt.; p<0.05; Fig. 4I) and consequently higher heart rate (CO 358.8 ± 9.56 vs SS 419.5 ± 13.91

bpm; p<0.05; Fig. 4J), without morphological alterations on cardiomyocytes (Fig. 4 K), or interstitial collagen deposition (Fig. 4L).

3.5. SS diet induces interscapular BAT hypertrophy but not whitening.

The SS group exhibited increased interscapular brown adipose tissue normalized weight (CO 65.47 ± 5.632 vs SS 194.6 ± 11.17 mg/100 g b.wt.; p<0.0001; Fig. 5A), as well as hypertrophy of brown adipocytes (CO 381.9 ± 17.97 *vs* SS 500.3 ± 41.11 μm^2; p<0,0001; Fig. 5B). Molecular analysis showed that BAT of the SS group had a strong trend of increasing β3 adrenoreceptors (p=0.0943; Fig. 5C), although no changes in the thermogenic protein UCP-1 (Fig. 5D). In addition, an increase in PPARα expression (CO 1.00 ± 0.1311 *vs.* SS 1.51 ± 0.1238% of control; p<0.05; Fig. 5E) without changes in PPARγ, AKT, or the pAKT-to-AKT ratio (Fig. 5F-H) was observed in SS animals compared to that in CO.

4. DISCUSSION

Here, we evaluated the early effects of high-sodium and high-sucrose intakes during puberty and early adulthood on the health status of Wistar rats. Surprisingly, we found that the SS diet affected energy intake, leading to lower protein intake, leading to lower lean mass and increased fat accumulation in the adipocytes and liver due to high carbohydrate intake. In addition to metabolic impairment, glucose homeostasis was not affected. There was impaired creatinine clearance in the kidney due to a reduced glomerular filtration rate and urinary flux. In the heart, the SS diet affected heart rate but not morphology. Like white adipose tissue, brown adipose tissue was hypertrophied; however, PPARα was upregulated, supporting the tissue morphology.

In our study, the SS group had a lower body weight and food intake than the CO group, in contrast to the higher SS consumption. Notably, the forced consumption of a solution containing a high concentration of sodium and sucrose instead of tap water will increase the liquid consumption owing to the high osmolarity of the solution and consequent increase in plasma osmolarity, which activates thirst mechanisms. Interestingly, we observed a slight reduction in liquid consumption and hypothesized that this is a mechanism related to momentary aversion to elevated sodium and sucrose levels in the diet, as the same event tends to repeat itself in the last week of treatment. Moreira et al.[8] conducted a similar experimental design using the same sodium concentration in drinking water and found that

the experimental groups did not have reduced food intake. This suggests that, in our study, the reduction in food intake was caused by the high carbohydrate intake from the SS diet rather than sodium intake. In addition, owing to the lower food intake and consequent reduction in protein intake, the SS animals probably had sarcopenia, which decreased the basal metabolic rate and favored fat accumulation, as observed in our study. In contrast, animals fed a low-protein diet for one month during puberty presented lower fat than those in the control groups[29]. In the study by Oliveira et al.[29], despite high carbohydrate intake, the animals did not show adipose tissue hypertrophy, indicating that the source of carbohydrates can modulate fat accumulation because the source used by the authors was a mixture of sucrose and cornstarch. Surprisingly, both groups had similar Lee index, which mimics individuals with normal BMI but increased metabolic impairments [1,2,25]. Here, we analyzed the correlation between fat pad weight and body weight and found that the adipose tissue of the SS animals was positively correlated with body weight, similar to the CO group. Notwithstanding, the point of interception of the curves differed between the groups, showing that despite the lower body weight of SS animals, their adipose tissues were heavier than those of the CO groups. This result highlights fat accumulation in the SS group independent of body weight gain, revealing a skinny fat phenotype.

We did not observe any differences between the groups during the insulin and glucose tolerance tests, meaning the SS diet could not alter glucose homeostasis in the SS group. When we analyzed the pancreas morphology, we observed an increased normalized weight without pancreatic islet hypertrophy. We did not observe any signs of ectopic fat accumulation in the pancreas of the SS animals, and we attribute the increased relative pancreatic weight to slight variability in gross pancreatic weight among the animals. Although the SS diet did not affect glucose homeostasis, several studies have reported normoglycemia in the context of hyperinsulinemia [30–32]. While the combination of sodium and sucrose does not appear to disrupt glycemic balance directly, one study examining the association between soft drink consumption, weight gain, and DM reported that excessive consumption of these products contributes to increased body mass, raising blood glucose levels [33].

The liver is one of the organs most injured during high-carbohydrate consumption. In our model, we observed an increase in the normalized weight of the liver and microvesicular lipid inclusion. However, no differences in plasma markers of liver injury were observed, showing that despite the beginning of fat accumulation in the liver, there was no extensive

damage to the tissue. These results indicate a liver *de novo* lipogenesis alteration, which needs to be assessed in future studies. A study carried out in mice showed that an overload of 50% sucrose or 50% fructose for 15 weeks contributed to increased steatosis and elevated plasma levels of ALT and AST [4]. In addition to liver changes, a sucrose-rich diet leads to increased adiposity and weight gain compared with a fructose-rich diet[4].

The kidney is most injured during sodium or glucose overload [34–37]. In our study, we observed increased normalized weight of the kidney; however, a decrease in both glomerular and capsular space and pericapsular collagen decrease highlights the morphological effects of the SS diet in the experimental group. Similar to the morphological impact of the SS diet, kidney function was impaired, as shown by the lower creatinine clearance due to the reduced glomerular filtration rate and urinary flow. We observed a lower heart-to-body weight ratio in the heart, although no alterations in cardiomyocyte diameter and collagen deposition were observed. However, the SS animals had higher heart rates than the CO animals. Moreira et al.[28] showed that a high-sodium diet increases collagen deposition and impairs cardiac relaxation.

The higher the nutrient availability, the higher the input for adipocyte energy accumulation [38]. However, brown adipose tissue regulates energy expenditure because of its high metabolic activity under certain stimuli[22]. Adrenergic stimulus increases thermogenesis in the BAT through β3 receptor activation and the upregulation of uncoupling protein type 1 (UCP-1)[39]. Our study observed that the SS group had a higher normalized weight of BAT and brown adipocyte area. Even so, the adrenergic β3 receptor showed increased expression in the SS group, although no differences in UCP-1 expression were noted. In this context, hypertrophy of BAT is commonly linked to tissue whitening, which means the loss of mitochondrial function or number. Whitening leads to impaired thermogenesis and lipid handling in brown adipocytes, which function as a stock of lipids in unilocular vesicles instead of multilocular vesicles that facilitate lipid metabolism[21]. In our study, we did not observe any characteristics of BAT whitening in the SS group. PPARα is the primary protector against BAT whitening, mainly in animals fed high-fat diets[17,40]. PPARα is the primary regulator of adipose tissue energy expenditure and regulates genes involved in thermogenesis and catecholamine response [41]. In our study, SS animals had an increased amount of PPARα, which probably drives the maintenance of the brown-adipocyte phenotype. However, the SS diet did not affect PPARγ, the primary regulator of UCP

expression. To the best of our knowledge, this is the reason for hypertrophied brown adipocytes[42].

5. CONCLUSION

Altogether, our results show that an SS diet early in life affects body development by impairing white adipose tissue metabolism. In addition, the increase in *de novo* lipogenesis by the liver was partly buffered by brown adipose tissue metabolism, highlighting the protective role of BAT metabolism under the study conditions. Although BAT could not increase lipid consumption, the maintenance of the brown phenotype shows a protective role in the maintenance of sympathetic tone in this tissue. This experimental model resembles obesity-related symptoms that occur in people with an average body mass index and is a non-apparent obese model (skinny fat) for studying markers of metabolic syndrome, such as increased heart rate, liver lipid inclusion, impaired renal function, and increased adiposity.

Financial support

This research was funded by Fundação de Amparo à Pesquisa do Estado de Goiás - FAPEG grant numbers: 201710267000517-GRP, 201810267001636-GRP, 2022151000060-GRP; Conselho Nacional de Desenvolvimento Científico e Tecnológico - CNPq grant numbers: 447496/2014-0-GRP, 309989/2016-7-GRP, 312130/2019-8-GRP, 315335/2023-8-GRP; FAPESP/FAPEG grant number: 2019/24154-3; and Coordenação de Aperfeiçoamento de Pessoal de Nível Superior (CAPES).

Declaration of Interests

The authors declare that they have no conflicts of interest.
Data can be accessed upon request by the interested party to the corresponding author.

Authorship

Authors' credit role: KVNC: Conceptualization, Methodology, Investigation, Writing - Original Draft; **MDFJ**: Conceptualization, Methodology, Investigation, Writing - Review & Editing; **MCSM** – Conceptualization, Methodology, Investigation, Writing - Review & Editing; **SMM** – Writing - Review & Editing; **JOF** – Writing - Review & Editing; **RAM** – Resources, Writing - Review & Editing; **PCL** – Resources, Writing - Review & Editing;

EGM – Resources, Writing - Review & Editing; **CHX** – Writing - Review & Editing; **EC** – Supervision, Writing - Review & Editing; **RMG** – Conceptualization, Methodology, Writing - Review & Editing; **GRP** – Conceptualization, Methodology, Writing - Review & Editing. All authors have read and approved the final version of the manuscript.

REFERENCES

1. Williams R & Periasamy M (2020) Genetic and Environmental Factors Contributing to Visceral Adiposity in Asian Populations. *Endocrinol. Metab.* **35**, 681–695.
2. Foulis SA, Hughes JM & Friedl KE (2020) New Concerns About Military Recruits with Metabolic Obesity but Normal Weight ("Skinny Fat"). *Obesity* **28**, 223–223.
3. Monteiro CA, Moubarac J -C., Cannon G, et al. (2013) Ultra-processed products are becoming dominant in the global food system. *Obes. Rev.* **14**, 21–28.
4. Schultz A, Barbosa-Da-Silva S, Aguila MB, et al. (2015) Differences and similarities in hepatic lipogenesis, gluconeogenesis and oxidative imbalance in mice fed diets rich in fructose or sucrose. *Food Funct.* **6**, 1684–1691. Royal Society of Chemistry.
5. Rippe C, Berger K, Böiers C, et al. (2000) Effect of high-fat diet, surrounding temperature, and enterostatin on uncoupling protein gene expression. *Am. J. Physiol. Metab.* **279**, E293–E300.
6. Tenk CM & Felfeli T (2017) Sucrose and fat content significantly affect palatable food consumption in adolescent male and female rats. *Appetite* **118**, 49–59. Elsevier Ltd.
7. Rosa GB, Cavalet LC, De Melo ABS, et al. (2020) High salt intake during puberty leads to cardiac remodelling and baroreflex impairment in lean and obese male Wistar rats. *Br. J. Nutr.* **123**, 642–651.
8. Moreira MCSS, da Silva EF, Silveira LL, et al. (2014) High sodium intake during postnatal phases induces an increase in arterial blood pressure in adult rats. *Br. J. Nutr.* **112**, 1923–1932. Cambridge University Press.
9. Westin T, Nascimento B de AA, Fontes BN, et al. (2007) The influence of lipogenesis in the obesity in humans. *Rev. Bras. Prescrição e Fisiol. do Exerc.* **1**, 01–12.
10. Schutz Y (2004) Dietary fat, lipogenesis and energy balance. *Physiol. Behav.* **83**, 557–564.
11. Taskinen MR & Borén J (2015) New insights into the pathophysiology of dyslipidemia in type 2 diabetes. *Atherosclerosis* **239**, 483–495.
12. Zheng Y, Ley SH & Hu FB (2018) Global aetiology and epidemiology of type 2

diabetes mellitus and its complications. *Nat. Rev. Endocrinol.* **14**, 88–98. Nature Publishing Group.

13. Dai P, Harada Y & Takamatsu T (2015) Highly efficient direct conversion of human fibroblasts to neuronal cells by chemical compounds. *J. Clin. Biochem. Nutr.* **56**, 166–170.
14. Legeza B, Marcolongo P, Gamberucci A, et al. (2017) Fructose, glucocorticoids and adipose tissue: Implications for the metabolic syndrome. *Nutrients* **9**, 426.
15. Tandon P, Wafer R & Minchin JEN (2018) Adipose morphology and metabolic disease. *J. Exp. Biol.* **121**, jeb164970.
16. Braun K, Oeckl J, Westermeier J, et al. (2018) Non-adrenergic control of lipolysis and thermogenesis in adipose tissues. *J. Exp. Biol.* **121**, jeb165381.
17. Lehnig AC & Stanford KI (2018) Exercise-induced adaptations to white and brown adipose tissue. *J. Exp. Biol.* **121**, jeb161570.
18. De Almeida DL, Fabrício GS, Trombini AB, et al. (2013) Early overfeed-induced obesity leads to brown adipose tissue hypoactivity in rats. *Cell. Physiol. Biochem.* **32**, 1621–1630.
19. Šefčíková Z & Raček Ľ (2015) Effect of neonatal β3-adrenoceptor agonist CL 316,243 treatment on body fat accumulation and intestinal alkaline phosphatase activity in rats from reduced nests. *Folia Histochem. Cytobiol.* **53**, 307–313.
20. Jocken JWE, Goossens GH, Van Hees AMJ, et al. (2008) Effect of beta-adrenergic stimulation on whole-body and abdominal subcutaneous adipose tissue lipolysis in lean and obese men. *Diabetologia* **51**, 320–327.
21. Souza-Tavares H, Miranda CS, Vasques-Monteiro IML, et al. (2023) Peroxisome proliferator-activated receptors as targets to treat metabolic diseases: Focus on the adipose tissue, liver, and pancreas. *World J. Gastroenterol.* **29**, 4136–4155.
22. Jahansouz C, Xu H, Hertzel A V., et al. (2018) Partitioning of adipose lipid metabolism by altered expression and function of PPAR isoforms after bariatric surgery. *Int. J. Obes.* **42**, 139–146.
23. Sharma N, Okere IC, Barrows BR, et al. (2008) High-sugar diets increase cardiac dysfunction and mortality in hypertension compared to low-carbohydrate or high-starch diets. *J. Hypertens.* **26**, 1402–1410.
24. Ritze Y, Bárdos G, D'Haese JG, et al. (2014) Effect of high sugar intake on glucose transporter and weight regulating hormones in mice and humans. *PLoS One* **9**, 1–9.

25. Zhou X, Han D, Xu R, et al. (2014) A model of metabolic syndrome and related diseases with intestinal endotoxemia in rats fed a high fat and high sucrose diet. *PLoS One* **9**, e115148 [Volti GL, editor].

26. Hinojosa-Laborde C, Jespersen B & Shade R (2015) Physiology Lab Demonstration: Glomerular Filtration Rate in a Rat. *J. Vis. Exp.*

27. Ferreira-Junior MD, Cavalcante KVN, Costa JM, et al. (2024) Early Methylglyoxal Exposure Leads to Worsened Cardiovascular Function in Young Rats. *Nutrients* **16**, 1–15.

28. Moreira MC dos S, Nunes AD de C, Lopes PR, et al. (2024) Sodium overload during postnatal phases impairs diastolic function and exacerbates reperfusion arrhythmias in adult rats. *J. Dev. Orig. Health Dis.* **15**, e9.

29. de Oliveira JC, de Moura EG, Miranda RA, et al. (2018) Low-protein diet in puberty impairs testosterone output and energy metabolism in male rats. *J. Endocrinol.* **237**, 243–254.
30. Chen C, Hosokawa H, Bumbalo LM, et al. (1994) Mechanism of compensatory hyperinsulinemia in normoglycemic insulin- resistant spontaneously hypertensive rats. Augmented enzymatic activity of glucokinase in β-cells. *J. Clin. Invest.* **94**, 399–404.
31. Santos SHS, Fernandes LR, Mario ÉG, et al. (2008) Mas deficiency in FVB/N mice produces marked changes in lipid and glycemic metabolism. *Diabetes* **57**, 340–347.
32. Alwahsh SM, Dwyer BJ, Forbes S, et al. (2017) Insulin production and resistance in different models of diet-induced obesity and metabolic syndrome. *Int. J. Mol. Sci.* **18**.
33. Schulze MB, Manson JAE, Ludwig DS, et al. (2004) Sugar-sweetened beverages, weight gain, and incidence of type 2 diabetes in young and middle-aged women. *J. Am. Med. Assoc.* **292**, 927–934.
34. Kitada K, Daub S, Zhang Y, et al. (2017) High salt intake reprioritizes osmolyte and energy metabolism for body fluid conservation. *J. Clin. Invest.* **127**, 1944–1959.
35. Dobrian AD, Schriver SD, Lynch T, et al. (2003) Effect of salt on hypertension and oxidative stress in a rat model of diet-induced obesity. *Am. J. Physiol. - Ren. Physiol.* **285**, F619–F628.
36. Lanaspa MA, Kuwabara M, Andres-Hernando A, et al. (2018) High salt intake causes leptin resistance and obesity in mice by stimulating endogenous fructose production and metabolism. *Proc. Natl. Acad. Sci. U. S. A.* **115**, 3138–3143.
37. Rosca MG, Mustata TG, Kinter MT, et al. (2005) Glycation of mitochondrial proteins from diabetic rat kidney is associated with excess superoxide formation. *Am. J. Physiol. - Ren. Physiol.* **289**, F420–F430.
38. Breton C (2013) The hypothalamus-adipose axis is a key target of developmental programming by maternal nutritional manipulation. *J. Endocrinol.* **216**.
39. Collins S (2012) β-Adrenoceptor signaling networks in adipocytes for recruiting stored fat and energy expenditure. *Front. Endocrinol. (Lausanne).* **3**, 1–7.
40. Chen H, Tan H, Wan J, et al. (2023) PPAR-γ signaling in nonalcoholic fatty liver disease: Pathogenesis and therapeutic targets. *Pharmacol. Ther.* **245**, 108391. Elsevier Inc.
41. Pawlak M, Lefebvre P & Staels B (2015) Molecular mechanism of PPARα action and its impact on lipid metabolism, inflammation and fibrosis in non-alcoholic fatty liver disease. *J. Hepatol.* **62**, 720–733. European Association for the Study of the Liver.
42. Magliano DC, Bargut TCL, de Carvalho SN, et al. (2013) Peroxisome Proliferator-Activated Receptors-Alpha and Gamma Are Targets to Treat Offspring from Maternal Diet-Induced Obesity in Mice. *PLoS One* **8**.

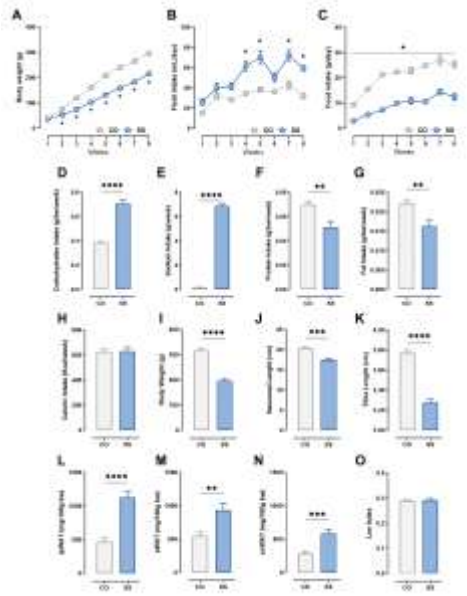

Figure 1. The SS diet affects body development and leads to an increase in adipose tissue weight. The SS group presented lower body weight gain (A), high fluid intake (B), and lower food intake (C) during the experimental period compared to the CO group. In the last week, the SS group presented increased carbohydrate and sodium intake (D-E) and reduced protein and fat intake (F-G) despite no alterations in overall caloric intake (H). This dietary pattern affected body weight (I), nasoanal length (J), and tibial length (K). However, SS animals presented increased retroperitoneal (rp), epididymal (e), and inguinal subcutaneous (sc) WAT adipose tissue (L-N) compared to CO animals. However, the Lee index (O), mainly used to indicate obesity in rats, was not altered. Two-way ANOVA was used for time-dependent analysis, and other analyses were performed using the Student's t-test (n=8 animals per group). *p<0.05, **p<0.01, ***p<0.001 and ****p<0.0001.

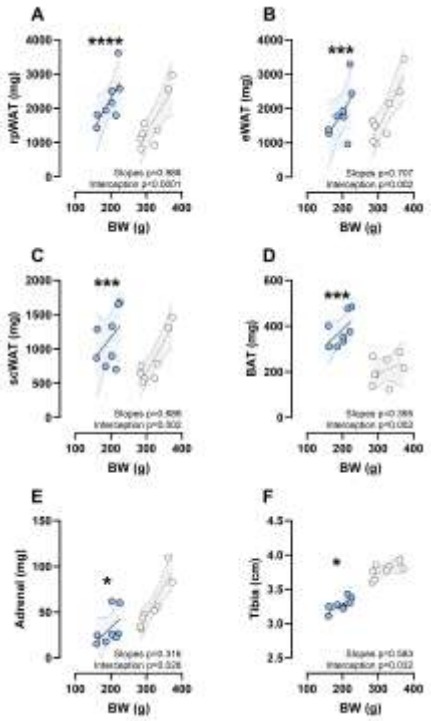

Fig. 2. The SS diet correlated with increased white and brown adipose tissue weights. Visceral (A-B) and subcutaneous (C) WAT and interscapular BAT (D) were correlated with BW, as observed in the CO group, although the SS group had left-displaced points. Inversely, as with adipose tissue, the adrenal gland (E) and tibia length (F) were weakly correlated with body weight. A simple linear regression was used (n= 8 animals per group). *p<0.05, ***p<0.001 and ****p<0.0001.

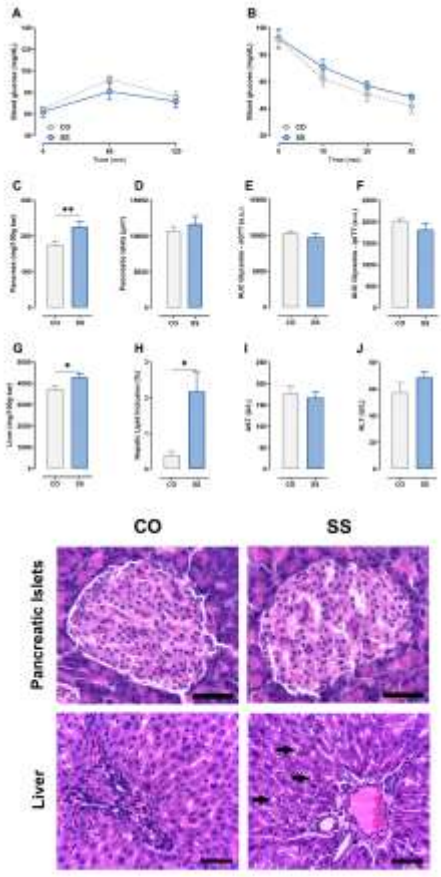

Fig. 3. SS diet does not affect glucose homeostasis but leads to hepatic lipid inclusion. At the end of the experimental period, no differences were detected during the oGTT (A, E) or ipITT (B, F). Despite the high pancreas-to-BW ratio in the SS group compared with the CO group, no difference was detected in the pancreatic islet area (D). The liver-to-BW ratio (G) and hepatic lipid content were higher in SS animals than in CO. However, no differences were detected in the plasma markers of liver injury (I-J). Two-way ANOVA was used for time-dependent analysis, and other analyses were performed using Student's t-test (n= 6-8 animals per group). *$p<0.05$ and **$p<0.01$. Representative photomicrographs of HE-stained slices of the pancreas and liver are shown at the bottom (black arrows indicate microvesicular lipid inclusion, while black bars indicate 50 μm).

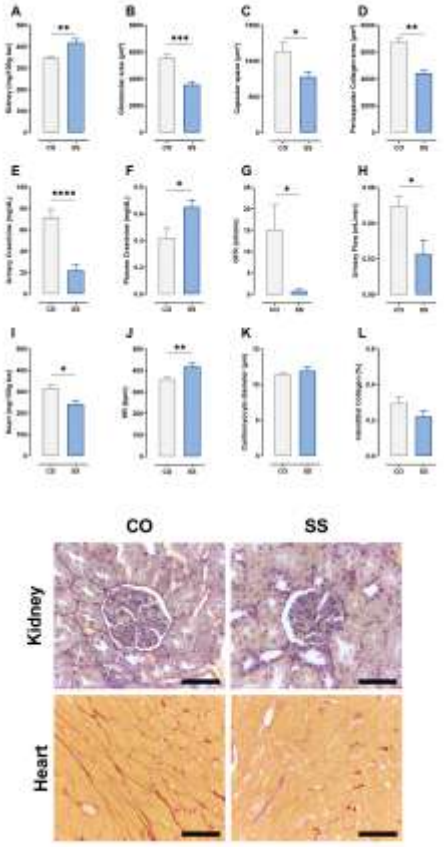

Fig. 4. The SS diet affects renal function and increases heart rate. Despite a higher kidney-to-BW ratio (A), the SS group showed a reduced glomerular area (B), capsular space (C), and pericapsular collagen (D) compared to the CO group. In addition, the SS diet shifts urinary-to-plasmatic creatinine levels (E-F), which represent an impaired glomerular filtration rate (G) and reduced urinary flow (H). Despite a lower heart-to-BW ratio (I), the SS animals showed an increased heart rate (J). However, no differences were observed in the cardiomyocyte diameter (K) or interstitial collagen deposition (L). The Student's t-test was used (n= 8 animals per group). *$p<0.05$, **$p<0.01$, ***$p<0.001$ and ****$p<0.0001$. Representative photomicrographs of picrosirius-red-stained slices of the kidney and heart are at the bottom (collagen in red; black bars measure 50 μm).

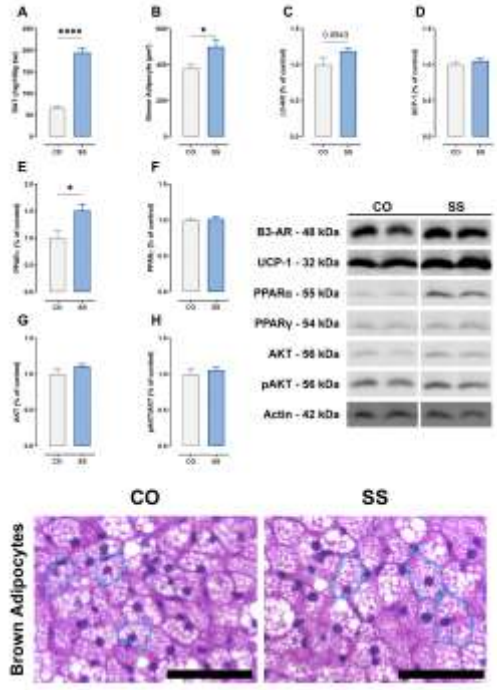

Fig. 5. The SS diet-induced interscapular BAT hypertrophy but not whitening. The SS group showed both whole BAT (A) and brown adipocyte hypertrophy (B), despite a slight increase in β3-AR (C), without UCP-1 (D) changes. Interestingly, PPARα (E) levels were higher in the SS group than in the CO group regarding protection against whitening. No differences were observed in PPARγ (F), AKT (G), and pAKT-to-AKT ratio (H). The Student's t-test was used (n= 4-8 animals per group). *$p<0.05$ and ****$p<0.0001$. Representative photomicrographs of HE-stained slices of BAT are at the bottom (brown adipocytes highlighted with a cyan dotted line; black bars measure 50 μm).